

# Microelastic gradient gelatinous gels to induce cellular mechanotaxis

Satoru Kidoaki<sup>a,\*</sup>, Takehisa Matsuda<sup>b</sup>

<sup>a</sup> Division of Biomolecular Chemistry, Institute for Materials Science and Engineering, Kyushu University, Fukuoka 819-0395, Japan

<sup>b</sup> Genome Biotechnology Laboratory, Kanazawa Institute of Technology, Ishikawa 924-0838, Japan

Received 10 January 2007; received in revised form 26 June 2007; accepted 1 August 2007

## Abstract

The understanding and realization of directional cell movement towards a harder region of a cell culture substrate surface, so-called mechanotaxis, might provide a solid basis for a functional artificial extracellular matrix, enabling manipulation and elucidation of cell motility. The photolithographic surface microelasticity patterning method was developed for fabricating a cell-adhesive hydrogel with a microelasticity gradient (MEG) surface using photocurable styrenated gelatin to investigate the condition of surface elasticity to induce mechanotaxis as a basis for such substrate-elasticity-dependent control of cell motility. Patterned MEG gels consisting of different absolute surface elasticities and elasticity jumps were prepared. Surface elasticity and its two-dimensional distribution were characterized by microindentation tests using atomic force microscopy (AFM). From analyses of trajectories of 3T3 cell movement on each prepared MEG gel, two critical criteria of the elasticity jump and the absolute elasticity to induce mechanotaxis were identified: (1) a high elasticity ratio between the hard region and the soft one, and (2) elasticity of the softer region to provide medium motility. Design of these conditions was found to be necessary for fabricating an artificial extracellular matrix to control or manipulate cell motility.

© 2007 Elsevier B.V. All rights reserved.

**Keywords:** Mechanotaxis; Cell motility; Microelastic gradient gel; AFM; Microindentation test; Styrenated gelatin

## 1. Introduction

Cell motility is a critical basis of various dynamical behaviors of the cell ensemble *in vivo*: inflammation (Parente et al., 1979a,b), wound healing (Martin, 1997), morphogenesis (Juliano and Haskill, 1993), and tumor metastasis (Berstein and Liotta, 1994), etc. Appropriate control of such biological processes has remained a longstanding goal of study in the fields of development of functional biomaterials and tissue engineering. Establishment of surface engineering of biomaterials to regulate cell motility is strongly required in those fields as well as understanding of its mechanisms.

If no stimuli to induce directional movement are given in the systems, amoeboid movements of adherent cells are generally a random-walk crawling process. Directional cell movements induced by various kinds of environmental stimuli have been known as cellular responses to gradients of dissolved chemicals (chemotaxis) (Carter, 1965); surface-fixed biomolecules (hap-

totaxis) (Carter, 1967); light intensity (phototaxis) (Saranak and Foster, 1997); electrostatic potential (galvanotaxis) (Erickson and Nuccitelli, 1984); gravitational potential (geotaxis) (Lowe, 1997); and surface elasticity (durotaxis or mechanotaxis) (Lo et al., 2000; Gray et al., 2003; Guo et al., 2006). From the perspective of development of functional biomaterial surfaces, haptotaxis and mechanotaxis are expected to be applicable for preparing an artificial extracellular matrix to manipulate cell motility because the nano/micro-distribution of surface-fixed biomolecules and surface elasticity can be designed using a bio-engineering approach. Although many studies have examined approaches using haptotaxis (Jung et al., 2001), application of mechanotaxis has not been performed sufficiently because an appropriate condition of surface microelasticity distribution to induce mechanotaxis has not been established.

For this study, we developed a photolithographic surface microelasticity patterning method using photocurable styrenated gelatin for fabricating a cell-adhesive hydrogel with a microelasticity gradient surface. We prepared a microelastic gradient (MEG) gel with different absolute surface elasticities and elasticity jumps to investigate conditions of surface microelasticity to induce mechanotaxis. Surface elasticity and its two-dimensional

\* Corresponding author. Tel.: +81 92 802 2507; fax: +81 92 802 2509.  
E-mail address: [kidoaki@ms.ifoc.kyushu-u.ac.jp](mailto:kidoaki@ms.ifoc.kyushu-u.ac.jp) (S. Kidoaki).

distribution were characterized by microindentation tests using atomic force microscopy (AFM). An analysis of cell trajectories facilitated by time-lapse observations extracted two important surface elasticity criteria to induce mechanotaxis on the elasticity jump and the absolute elasticity of MEG gels: (1) the high elasticity ratio between hard and soft regions and (2) the elasticity of the soft region to provide medium motility. The importance of these two criteria and basic mechanisms by which those conditions affect induction of mechanotaxis are discussed.

## 2. Materials and methods

### 2.1. Preparation of microelastic gradient gel

A vinyl-silanized glass substrate was prepared for chemically fixing the hydrogel with a microelastic gradient surface (MEG gel) according to the following procedures: (1) glass substrates (0.12–0.17 mm thickness, 15 mm diameter; Matsunami Glass Ind. Ltd., Osaka, Japan) were immersed in 80 °C piranha solution (conc. H<sub>2</sub>SO<sub>4</sub>: 30% H<sub>2</sub>O<sub>2</sub> = 7:3) for 1 h; (2) after sequential rinsing with distilled water (DDW), acetone and toluene, the glass substrates were immersed in 5% (v/v) toluene solution of vinyltrimethoxysilane (Tokyo Chemical Industry Co. Ltd., Tokyo, Japan), and shaken for 18 h at room temperature; (3) after sequential rinsing with toluene, acetone, ethanol and DDW, the glass substrate was dried at 115 °C for 10 min in air.

Using photocurable styrenated gelatin that we had synthesized previously, MEG gel was prepared photolithographically (Okino et al., 2002) (see experimental setup shown in Fig. 1): (1) 40 wt.% phosphate buffered saline (PBS) solution of styrenated gelatin (degree of derivatization: 76.1%) with water-soluble carboxylated camphorquinone (Okino et al., 2002) (0.1 wt.% of gelatin) was spread between the vinyl-silanized glass substrate and the raw substrate; (2) visible light with intensity of 140 mW/cm<sup>2</sup> (measured at 514 nm) was irradiated for 10–15 s on the styrenated gelatin sol from the backside of the vinyl-silanized glass substrate through an unilateral photomask with 20% light transmittance (5 nm chromium-deposited glass substrate, transmitted light intensity: 28 mW/cm<sup>2</sup>). A metal halide

light source (MME-250; Moritex Corp., Tokyo, Japan) was used. Light intensity was measured using a laser power meter (HP-3; Pneum Co. Ltd., Saitama, Japan); (3) finally, the resultant MEG gel was detached from the raw glass substrate in PBS and subsequently immersed in PBS overnight to remove unreacted sol and make it swell sufficiently.

### 2.2. Measurement of surface elasticity of MEG gel

Surface elasticity and its distribution around the elasticity boundary on the MEG gel were determined using microindentation analysis. The force-indentation ( $f-i$ ) curves of the MEG gel surface were measured using AFM (NVB100; Olympus Optical Co. Ltd., Tokyo, Japan; AFM controller & software, Nanoscope IIIa; Veeco Instruments, CA, USA) along with a commercial silicon-nitride cantilever with a half-pyramidal tip and nominal spring constant of 0.03 N/m (Bio-lever; Olympus Optical Co. Ltd.) in PBS at three randomly chosen points in each position parallel to the boundary ( $n=3$ ) of three different samples ( $n=3$ ). The frequency of the tip approach/retract cycle was chosen as 1.5 Hz to minimize the noise fluctuation in a single  $f-d$  curve. Young's moduli of the surface were evaluated from  $f-i$  curves by nonlinear least squares fitting to the Hertz model in the case of a conical indenter (Hertz, 1881; Sneddon, 1965)

$$F = \frac{2 \tan(\alpha)}{\pi} \frac{E}{1 - \mu^2} \delta^2 \quad (1)$$

where  $F$  is the load,  $\delta$  the indentation depth,  $E$  Young's modulus,  $\mu$  the Poisson ratio and  $\alpha$  is a semivertical angle of the indenter. In this study,  $\alpha$  and  $\mu$  were assumed respectively as 30° and 0.5.

### 2.3. Cell culture

The mouse fibroblast cell line (3T3-Swiss albino) purchased from Dainippon Pharmaceutical Co. Ltd. (Osaka, Japan) was cultured in Dulbecco's modified Eagle's medium (DMEM; Gibco BRL, Grand Island, NY, USA) supplemented with 10% fetal bovine serum (FBS; Gibco BRL), 3.5 g/l glucose, 2 mM L-glutamine, 100 units/ml penicillin and 100 µg/µl streptomycin. Cells were maintained on tissue culture polystyrene dishes at 37 °C under 5% CO<sub>2</sub> in a humidified incubator.

### 2.4. Time-lapse analysis of cell migration

The migratory behavior of cells on MEG gel surface was monitored using a time-lapse image-capturing system (Himawari; Library Inc., Tokyo, Japan) connected to a phase-contrast microscope (IX70; Olympus Optical Co. Ltd., Tokyo, Japan) with a temperature and humidity controllable cell chamber (MATS-CO2CHK; TOKAI HIT, Shizuoka, Japan). Prior to the time-lapse recording experiment, cells were seeded at a density of  $1.5 \times 10^4$  cells/cm<sup>2</sup> on MEG gel and cultured with DMEM containing 10% FBS under 5% CO<sub>2</sub> for 7 h. Then, DMEM was exchanged with L15 (Gibco BRL) containing 10% FBS to adapt the cultured cells to the long observation period without needing to regulate CO<sub>2</sub> concentration in our cell chamber. Images of cells were captured every 15 min for 20 h. The

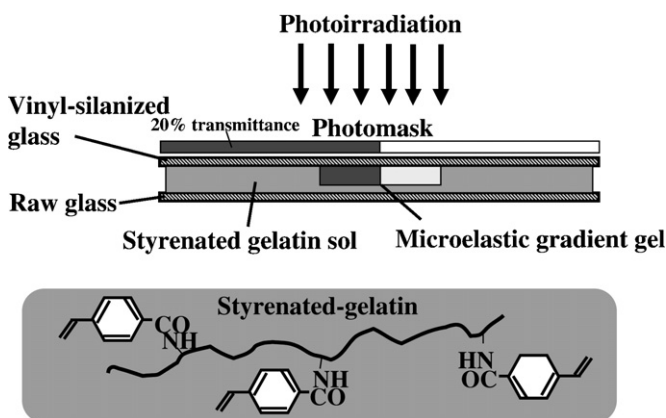


Fig. 1. Experimental setup for preparation of microelastic gradient gels using photolithographic surface elasticity patterning with photocurable styrenated gelatin.

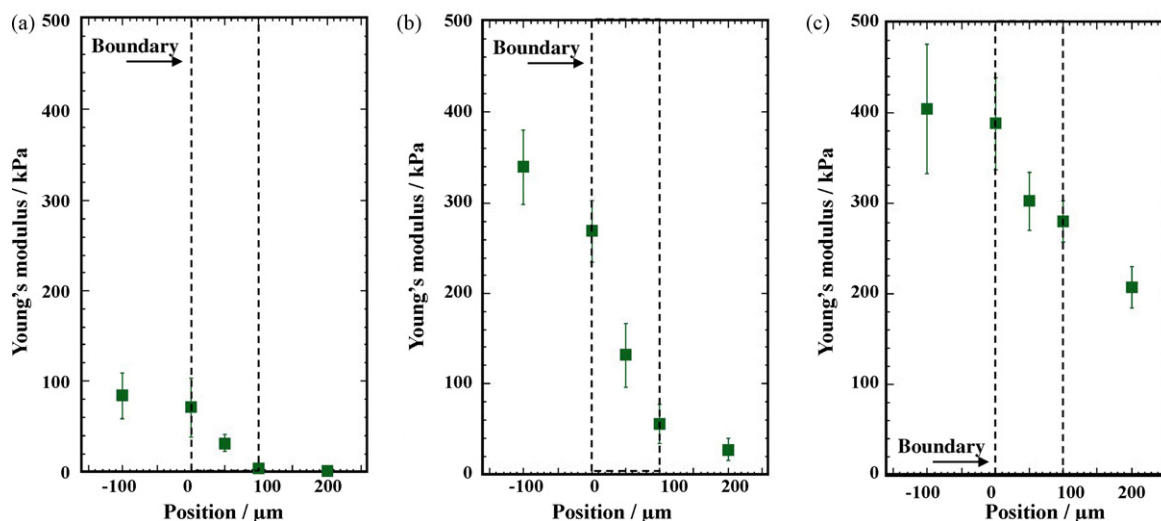


Fig. 2. Elasticity distribution around the elastic boundary in the MEG gel prepared under conditions of photoirradiation of 11 s (a), 12 s (b) and 15 s (c). Young's moduli were measured at three randomly chosen points in each position parallel to the boundary ( $n = 3$ ), and for three different samples ( $n = 3$ ). Average and standard deviations of Young's moduli in each position were determined from nine measurements.

coordinates of 20 isolated cells were measured using digitizing software and the positions of their nuclei. The migratory track and the moving speed were calculated from the coordinates; cell trajectories were presented in circular diagrams with the starting point of each trajectory situated in the diagram center.

### 3. Results

#### 3.1. Microelastic gradient gels with different surface elasticity conditions

To investigate the conditions of absolute elasticity and elasticity jumps to induce mechanotaxis, three different MEG gels with different surface elasticity conditions were prepared by changing photoirradiation periods: 11 s, 12 s and 15 s. Fig. 2 shows the elasticity distribution around the elasticity boundary on the prepared MEG gels, which was determined by AFM microindentation analysis based on a Hertz model. Photoirradiation of 11 s onto photocurable styrenated gelatin sol through a unilateral photomask produced an MEG gel with a ca. 80 kPa Young's modulus jump from the softer region with 10 kPa via a 100 μm gradient region (Fig. 2a, termed as gel A below). Similarly, photoirradiation of 12 s and 15 s produced MEG gels with a ca. 300 kPa jump from the softer region with 50 kPa (Fig. 2b, termed as gel B), and with a ca. 200 kPa jump from the softer region with 200 kPa (Fig. 2c, termed as gel C). Gel B exhibited the highest elasticity jump. Although the Young's moduli of hard and soft regions in each MEG gel increased with increased photoirradiation length, the degree of increase was reduced in harder regions of gel C. Due to 20% transmittance of the photomask used and inevitable diffusion of photocuring radical generator around mask boundary in the present experimental setup, it could not be realized to change the elasticity of only one side while fixing that of the other side. The elasticity of softer regions on gels A and B were prepared to roughly comparable levels (ca. 10 kPa and 50 kPa). Therefore, the sample set of gels A and B was used

for comparison to elucidate the effects of elasticity jumps from the same level elasticity surface on the cell movement. On the other hand, the sample set of gels B and C, which have harder regions with comparable levels of elasticity (ca. 350 kPa and 400 kPa), was applied for checking the effects of soft base elasticity of the cell movement onto the harder surface with similar elasticity.

#### 3.2. Cell movement observed on MEG gels

Cell movement on the prepared MEG gels was observed in a time-lapse manner with a 15 min interval. Fig. 3 shows the typical cell movement observed in the elasticity boundary on gel A, which was reconstructed from the extracted images with a 1.5 h interval for quick viewing. Exemplary numbered cells exhibited movement toward the harder region over the elasticity boundary between 10 h and 23.5 h after seeding. It is noteworthy that cell nos. 1 and 3 changed to a spindle shape parallel to the boundary and were unable to return to the softer region once they entered the harder region, which is a typical characteristic of mechanotaxis (Lo et al., 2000).

Trajectories of cell movement observed on soft, boundary and hard regions on the prepared MEG gel are shown in Fig. 4. The trajectories on all soft and hard regions showed isotropic distributions irrespective of conditions of the MEG gel (soft region, Fig. 4a and b; hard region, Fig. 4f–h). On gel C, the trajectories showed an isotropic distribution irrespective of the region (Fig. 4b, e and h); greatly biased trajectories towards the harder region were observed in the boundary region on gels A and B (Fig. 4c and d): mechanotaxis was observed.

Parameters to characterize cell migration were calculated for each trajectory and were compared to evaluate the effects of MEG conditions on induction and regulation of mechanotaxis (Fig. 5). Calculated migration parameters were (1) total migration distance (TMD), contour length of the trajectory; (2) track velocity (TV), velocity along the contour; (3) net translocation

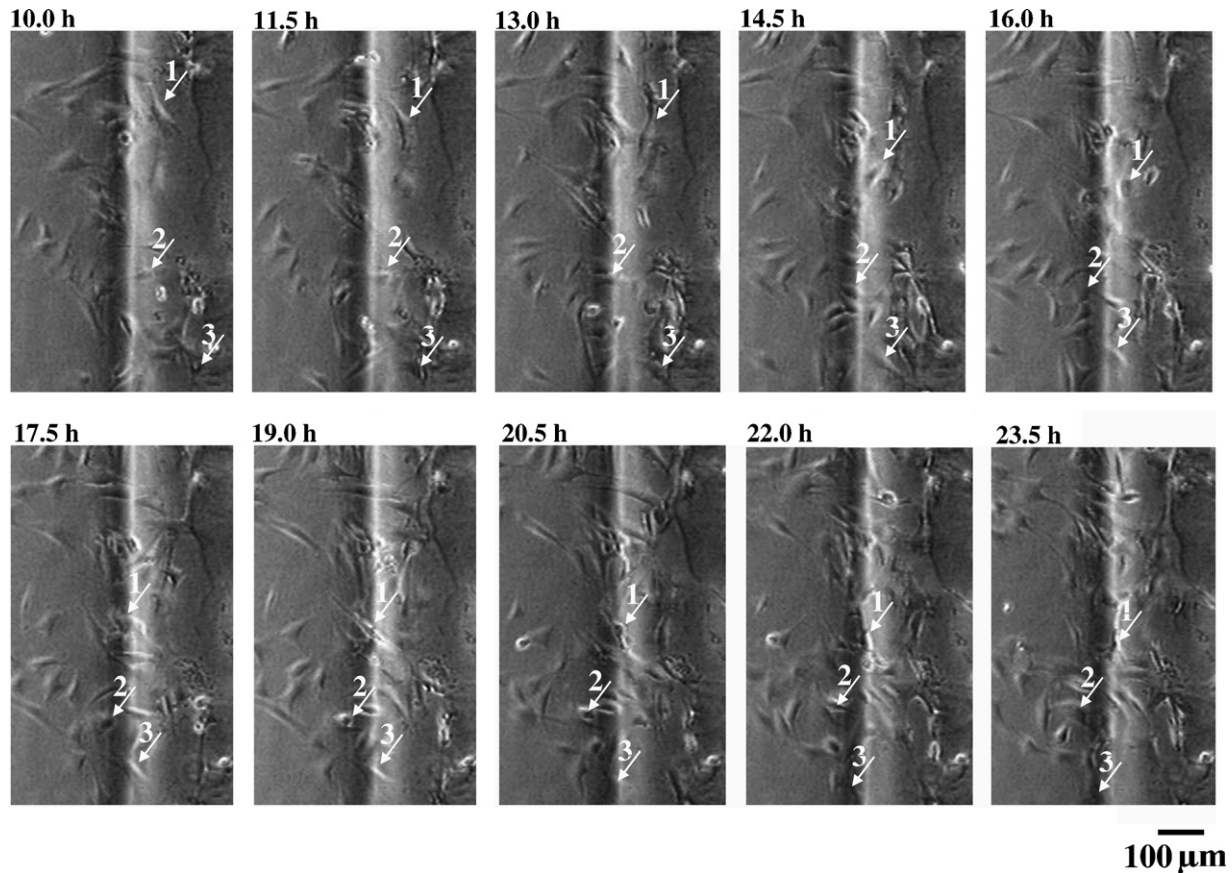


Fig. 3. Time-lapse observations of 3T3 cell movement in the elasticity boundary on the MEG gel A. Extracted images with 1.5 h interval from 10 h after seeding. Exemplary cells are numbered as 1–3.

distance (NTD), distance between the starting point and ending point; (4) net translocation velocity (NTV), velocity along the NTD; and (5) migration index (MI), the ratio of NTD to TMD, which expresses the linearity of the movement. As the Young's modulus of the soft base region increased from gels A–C, the longest and fastest movement was observed for gel B, followed by gels A and C (Fig. 5a and b). The MI shows the decreasing tendency from gels A–C, indicating that the soft gel region is rather effective in inducing a linear movement (Fig. 5c). Although gel B exhibited the most active movement in terms of migration distance and velocity, gel A showed dominance in the directional movement to the harder region from the perspective of MI or linearity of movement.

#### 4. Discussion

In this study, to investigate the conditions of surface elasticity distribution in an extracellular milieu to induce or regulate mechanotaxis, cell-adhesive hydrogels with a well-defined gradient of different microelasticities were prepared, and the cell behaviors on the hydrogels were analyzed. Below, we discuss the observed cellular responses on each MEG gel and define the critical criteria for inducing mechanotaxis from the mechanobiological viewpoint for designing an artificial extracellular matrix to manipulate cell motility.

Table 1 summarizes the cellular responses of velocity, the migration index and the degree of mechanotaxis on three MEG gels. First, the most effective induction of mechanotaxis was observed on gel A, which had a 10 kPa soft base region and an 80 kPa elasticity jump, and exhibited medium velocity. Second, the higher the ratio of elasticity between hard and soft regions (the H/S ratio), the more efficient mechanotaxis was observed. For instance, although the elasticity jump itself was smaller on gel A than on gel B, mechanotaxis was induced more efficiently on gel A, with the higher H/S ratio of 9, than on gel B with the H/S ratio of 7. Third, as the base elasticity increases from 10 kPa to 50 kPa to 200 kPa, high-velocity movement was observed on gel B, with the middle elasticity, and mechanotaxis was suppressed. Fourth, for the base region of the highest elasticity, movement itself was suppressed remarkably: mechanotaxis ceased even though the elasticity jump was a sufficiently high 200 kPa.

These results suggest that induction of mechanotaxis depends not only on the magnitude of the elasticity jump in the elastic-

Table 1  
Summary of the cell motility responses observed on the MEG gels A–C

|       | Base (kPa) | Jump (kPa) | H/S ratio | Velocity | MI     | Mechanotaxis |
|-------|------------|------------|-----------|----------|--------|--------------|
| Gel A | 10         | 80         | 9         | Middle   | High   | Strong       |
| Gel B | 50         | 300        | 7         | High     | Middle | Middle       |
| Gel C | 200        | 200        | 2         | Low      | Low    | –            |



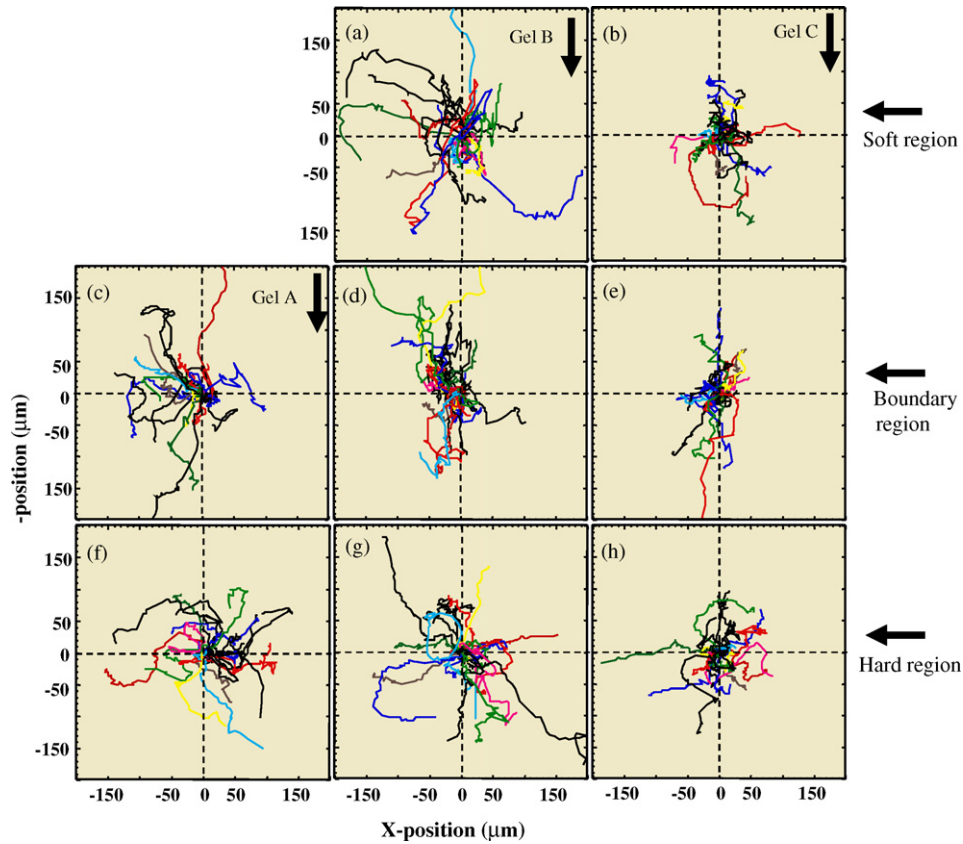


Fig. 4. Trajectories of 3T3 cell movement in each region of soft (a and b), boundary (c–e) and hard (f–h) on the prepared MEG gel A (c and f), B (a, d and g) and C (b, e and h) measured from time-lapse observations with a 15 min interval for 20 h from 7 h after seeding. Seeding density:  $1.5 \times 10^4$  cells/cm<sup>2</sup>. The softer region of gel A was so soft that a large fraction of the area was invariably detached from the vinyl-silanzed glass and the trajectories of many cells were not measurable. The starting position of each cell was set at the origin ( $n = 20$ ).

ity boundary region but also on the cellular motility regulated by elasticity on both harder and softer regions. The induction efficiency was considered to be affected by the balance between the former and the latter factors. Especially, the elasticity jump in the boundary region with the high H/S ratio and elasticity of base region to provide medium motility such as that on gel A

was verified as effective to induce efficient mechanotaxis. Actually, previous reports showed that mechanotaxis was induced for an elasticity jump from the softer region to the harder region, such as from 1.8 kPa to 34 kPa (Gray et al., 2003), from 12 kPa to 2.5 MPa (Gray et al., 2003), and from 14 kPa to 30 kPa (Lo et al., 2000). Those precedent studies used H/S ratios of 20,

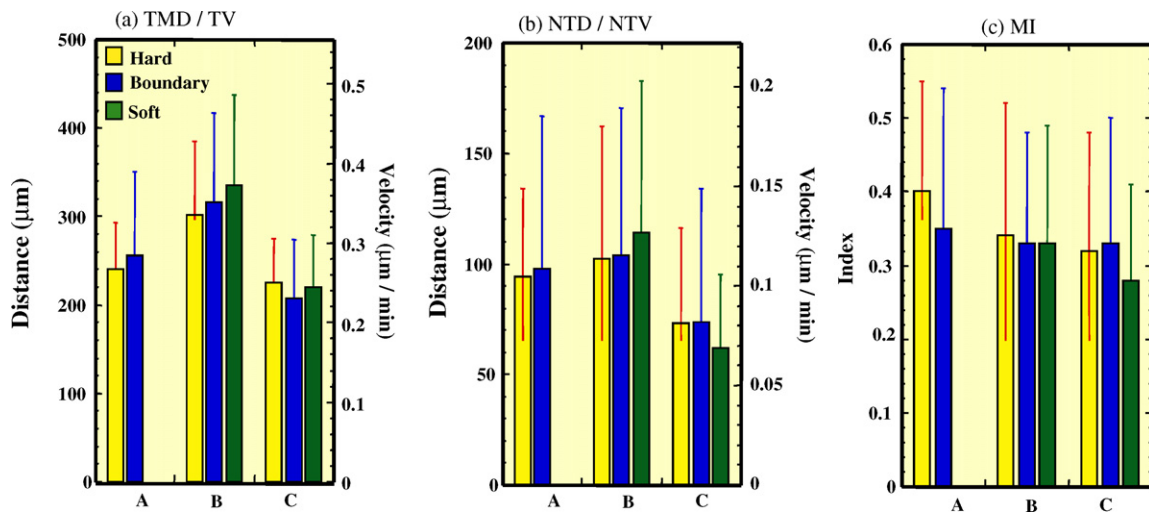


Fig. 5. Migration parameters calculated from the trajectories of cell movement shown in Fig. 4. (a) Total migration distance (TMD) and track velocity (TV). (b) Net translocation distance (NTD) and net translocation velocity (NTV). (c) Migration index (MI). Definitions for each parameter are given in the text. Error bars show standard deviations.

200 and 3 respectively, and the base elasticity was less than ca. 15 kPa, which is comparable to the elasticity level of gel A in this study.

A high H/S ratio can cause a considerable imbalance of traction forces generated at the focal adhesion (FA) sites in the adhered interface between the FA complexes located in harder and softer regions because the high elasticity surface withstands a large traction force and induces lateral strain well; the low one engenders elastic breakdown of FA complexes under the same traction force. Because the degree of that imbalance is greater, the driving force for mechanotaxis is stronger. On the other hand, elasticity providing medium motility is effective for cells to find the boundary more rapidly for imposing the above-mentioned directional movement in the intrinsic process of random-walk cellular movement. In general, reduced cell motility is observed on a very hard substrate. An overly hard surface adheres firmly to the cells and inhibits their motility, which lowers the probability of cells reaching the boundary.

From a mechano-biological viewpoint, *controlled mechanotaxis* is useful for designing an artificial extracellular matrix to manipulate cell motility. Design of both the microelastic jump and gradient with a high H/S ratio and absolute base elasticity to provide medium cellular motility were found to be critical factors for inducing mechanotaxis.

## 5. Conclusion

In this study, microelastic gradient gels were developed using photolithographic surface elasticity patterning with photocurable gelatin. The effects of the surface elasticity gradient to induce cellular mechanotaxis were investigated on those MEG gels. Results identified two critical design criteria of surface elasticity inducing mechanotaxis: (1) the magnitude of the elasticity jump and a gradient with a high H/S ratio and (2) the absolute base elasticity to provide medium cellular motility. Incorporation of these micro-gradient surface elastic properties into developing a mechano-active artificial extracellular matrix is essential to control or manipulate cell motility.

## References

- Berstein, L.R., Liotta, L.A., 1994. Molecular mediators of interactions with extracellular matrix components in metastasis and angiogenesis. *Curr. Opin. Oncol.* 6, 106–113.
- Carter, S.B., 1965. Principles of cell motility: the direction of cell movement and cancer invasion. *Nature* 208, 1183–1187.
- Carter, S.B., 1967. Haptotaxis and the mechanism of cell motility. *Nature* 213, 256–260.
- Erickson, C.A., Nuccitelli, R., 1984. Embryonic fibroblast motility and orientation can be influenced by physiological electric fields. *J. Cell Biol.* 98, 296–307.
- Gray, D.S., Tien, J., Chen, C.S., 2003. Repositioning of cells by mechanotaxis on surfaces with micropatterned Young's modulus. *J. Biomed. Mater. Res.* 66A, 605–614.
- Guo, W.-H., Frey, M.-T., Burnham, N.A., Wang, Y.-L., 2006. Substrate rigidity regulates the formation and maintenance of tissues. *Biophys. J.* 90, 2213–2220.
- Hertz, H., 1881. Ueber die Berührung fester elastischer Körper. *J. Reine Angew. Mathematik* 92, 156–171.
- Juliano, R.L., Haskill, S., 1993. Signal transduction from the extracellular matrix. *J. Cell Biol.* 120, 577–585.
- Jung, D.R., Kapur, R., Adams, T., Giuliano, K.A., Mrksich, M., Craighead, H.G., Taylor, D.L., 2001. Topographical and physicochemical modification of material surface to enable patterning of living cells. *Crit. Rev. Biotech.* 21, 111–154.
- Lo, C.-M., Wang, H.-B., Dembo, M., Wang, Y.-L., 2000. Cell movement is guided by the rigidity of the substrate. *Biophys. J.* 79, 144–152.
- Lowe, B., 1997. The role of  $Ca^{2+}$  in deflection-induced excitation of motile, mechanoresponsive balancer cilia in the ctenophore statocyst. *J. Exp. Biol.* 200, 1593–1606.
- Martin, P., 1997. Wound healing: aiming for perfect skin regeneration. *Science* 276, 75–81.
- Okino, H., Nakayama, Y., Tanaka, M., Matsuda, T., 2002. *In situ* hydrogelation of photocurable gelatin and drug release. *J. Biomed. Mater. Res.* 59, 233–245.
- Parente, L., Koh, M.S., Willoughby, D.A., Kitchen, A., 1979a. Studies on cell motility in inflammation. I. The chemotactic activity of experimental, immunological and non-immunological, inflammatory exudates. *Agents Actions* 9, 190–195.
- Parente, L., Koh, M.S., Willoughby, D.A., Kitchen, A., 1979b. Studies on cell motility in inflammation. II. The *in vivo* effect of anti-inflammatory and anti-rheumatic drugs on chemotaxis *in vitro*. *Agents Actions* 9, 196–200.
- Saranak, J., Foster, K.W., 1997. Rhodopsin guides fungal phototaxis. *Nature* 387, 465–466.
- Sneddon, I.N., 1965. The relation between load and penetration in the axisymmetric Boussinesq problem for a punch of arbitrary profile. *Int. J. Eng. Sci.* 3, 47–57.